IRANIAN JOURNAL OF PHYSICS RESEARCH

Iranian Journal of Physics Research, Vol. 16, No. 3, 2016

Research note

Compression between ion and hard x-ray emissions from nitrogen and argon in Mather type plasma focus device

S Paghe[1], M R Abdi[2], and B Shirani[1]

1. Department of Nuclear Engineering, Faculty of Advanced Sciences and Technologies, University of Isfahan, Isfahan, Iran
2. Department of Physics, Faculty of Science, University of Isfahan, Isfahan, Iran

E-mail: r.abdi@phys.ui.ac.ir

(Received 6 June 2014 ; in final form 13 April 2016)

Abstract

In this study, some characteristics of a Mather type Plasma Focus (PF) device such as a discharge current, pinch time, ion flux and hard x-ray intensity has been investigated simultaneously in argon and nitrogen gases separately for various operating gas pressures and charging voltages of capacitor bank. It was observed that pinch phenomena was energy and pressure dependent in current sheath as well as ion and hard x-ray emission intensity. Optimum pressure with maximum ion flux and the most intense hard x-ray showed a nearly linear dependence on the charging voltage of the device. Maximum ion flux was estimated in the order of 10^{18} ions per steradian in both gases. Hard x-ray emission was registered a little after discharge current and Faraday cup (FC) signals. Also, optimum pressure for maximum ion flux was not the same as the pressure for intense hard x-rays. Hard x-ray intensity reached its peak at higher pressures.

Keywords: Plasma Focus (PF), pinch time, ion flux, Faraday Cup (FC), hard x-ray

1. Introduction

Invention of novel PF devices by Mather [1] and Fillipov [2] independently opens a new era in nuclear science especially in radiation production sources and fusion plasma fields. PF devices have the potential to generate different types of charged particles such as ions and electrons in a broad energy ranging from several keV up to several tens of MeV [3-5], fusion neutrons (when deuterium is used as working gas), hard and soft x-rays as well as ultra violet lights [1-5]. In a Mather configuration, this device consists of two coaxial electrodes - inner and outer electrodes as the anode and cathode respectively- separated by an insulator and connected to a capacitor bank. By discharging the capacitor bank energy through the electrodes, gases near the anode ionize and electrical breakdown develops on the surface of the insulator. When two electrodes connect together electrically, the current sheath forms and accelerates particles by the effect of Lorentz force along the axis. By reaching the current to the open end of the anode, the radial collapse happens and a pinched plasma zone forms. This region is characterized by the formation of a dense, short-lived and energetic plasma. In this zone, strong electric fields are generated and the richest source of mentioned emissions is reported. Property studies of plasma formation and beam emission phenomena could lead to useful information about plasma behavior, fusion reactions and neutron production. Among the PF emissions, ion beams have been more appealing to the researchers because of their increasing applications in technology as well as their inevitable roles in the future of fusion reactors. Pulsed ion beam formation and acceleration properties in PF devices have been studied by several authors since the invention of PF devices [6-15]. Bernstein [6] studied ion acceleration in time-varying electromagnetic fields that are induced by plasma sheath acceleration. This mechanism was explained as a surfatron acceleration by Katsouleas and- Dawson [7]. Haines [8] investigated ion beam generation as a result of the emergence of m=0 instability and noticed its role in neutron production. Ion beams from PF devices are used in some technical and industrial applications such as ion implantation, surface modification, and so on [16-24]. Several diagnostic tools have been employed for ion beam monitoring such as Faraday Cups (FCs), Solid State Nuclear Track Detectors (SSNTD) and Thomson Parabola (TP) [25-28]. Kelly et al. [27] measured nitrogen ion's energy

Figure 1. Experimental set up.

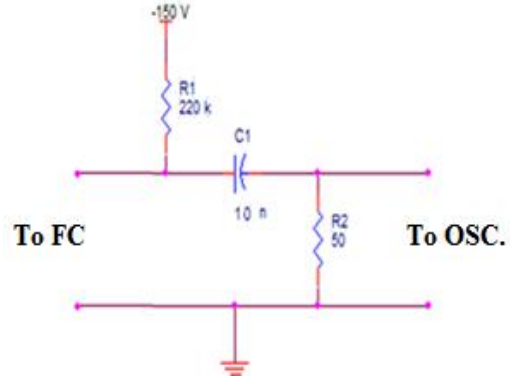

Figure 2 . Biasing circuit of the faraday cup.

with a FC assembly and Time of Flight technique (TOF). Etaati et al., [28] reported high dependence of argon ion flux and angular distribution on gas pressure and device energy. In their study, ion beam intensity decreased at angles larger than ±11 degrees but hard x-ray intensity showed a bimodal distribution with peaks around ±15 degrees. Also in another work, Bhuyan et al., [29] found a strong dependence of ion flux and angular distribution on working gas pressure. The time correlation between ion and x-ray emissions was studied by Yamamoto et al., [30] and Heo et al., [31]. According to their studies, ion beam and hard x-ray were not emitted simultaneously. Hard x-ray was monitored a little after ion beam emissions. This paper is an experimental report on PF ion beam and hard x-ray measurement. The paper was aimed to characterize these beams and their time correlation with pinch phenomena in different experimental conditions.

2. Experimental setup

All experiments were performed by a Mather type PF device with a capacitor bank C_0=9 μF and a specific charging voltage from 18.0±0.1 to 24.0±0.1 kV with a 2.0 kV pace interval. The device's electrodes consisted of a copper rode as anode (2.6 cm in diameter and 13.9 cm in length) and another six copper rods as cathode (each about 1 cm in diameter and 14.9 cm in length). Cathode rods are located in circumference of a circle with 3.95 cm in radius. Electrodes are located in a cylindrical stainless steel vacuum chamber of 32 cm in height and 19.4 cm in diameter. The experimental setup is shown in figure 1. Discharge current, ion flux and hard x-ray intensity of the device were monitored simultaneously by Rogowski coil, FC assembly and BC-400 scintillation detector respectively. The FC diagnostic was placed at 8 cm above the anode tip. The FC has been biased in a negative voltage so that it removes all the accompanied electrons from the incident ion beams. Also, negative biasing collects all the generated secondary electrons completely. To achieve this goal, the bias circuit in figure 2 was employed. Also for minimizing backscattering and secondary emissions, a pin hole was placed at the entrance of the cup. Hard x-ray intensity was measured by BC-400 scintillation detector. This diagnostic tool was biased with -1500 Volt and was placed one meter away from the anode in front of the vessel window.

3. Results

The results of the experiments in argon and nitrogen gases are presented separately in the following subsections.

3.1. Argon gas

Discharge current and pinch time behavior with the device energy are depicted in figure 3. This curve is plotted at 0.40±0.01 mbar. According to the graphs, when the charging voltage increases, the pinch phenomena happens sooner because of the reduction in axial and radial sweep time of the plasma sheath. In fact, the current sheath velocity has a direct dependence on the device energy. This result can be explained by theoretical relations of Lee model [32].

$$t_a = \left[\frac{4\pi(c^2-1)}{\mu_0\ lnc}\right]^{\frac{1}{2}} \cdot \frac{\sqrt{f_m}}{f_c} \cdot \frac{Z_0}{\frac{I_0}{a}\Big/\sqrt{\rho_0}},$$

$$t_r = \frac{4\pi}{\left[\mu_0(\gamma+1)\right]^{\frac{1}{2}}} \cdot \frac{\sqrt{f_{mr}}}{f_{cr}} \cdot \frac{a}{\frac{I_0}{a}\Big/\sqrt{\rho_0}},$$

where t_a and t_r are characteristic axial and radial transit times of plasma focus dynamics. In this equation, Z_0 and a are the length and the radius of anode respectively. (c= ln (b/a), b is the cathode distance from the anode axis). The f_m and f_{mr} are the mass swept-up factors and f_c and f_{cr} are the current drive fractions respectively in axial and radial phases. According to the equations, in a constant pressure, by increasing the device energy, I_0 reaches to a higher value, so t_a and t_r decreases. As a result, the pinch of the current sheath occurs sooner. In other words, the more energy applied to the electrodes, the sooner pinch is got. The emergence of MHD instabilities generates strong electric fields in plasma column, so charged

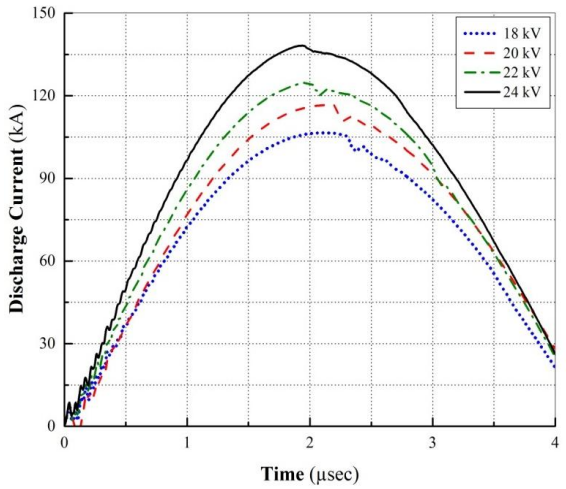

Figure 3. Variation of discharge current with time for argon (All plots are obtained with 0.40 mbar gas pressure).

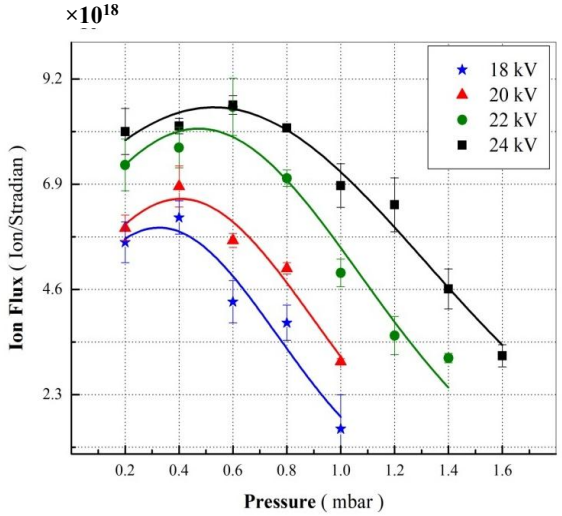

Figure 4. Ion flux variation vs. gas pressure in different charging voltages for argon.

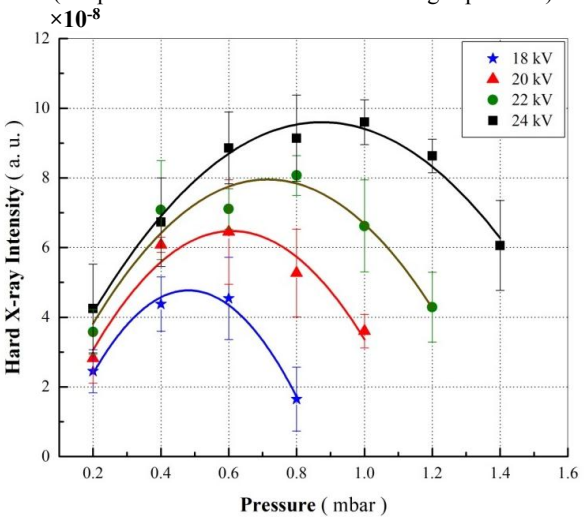

Figure 5. Hard x-ray intensity vs. gas pressure in different charging voltage for argon.

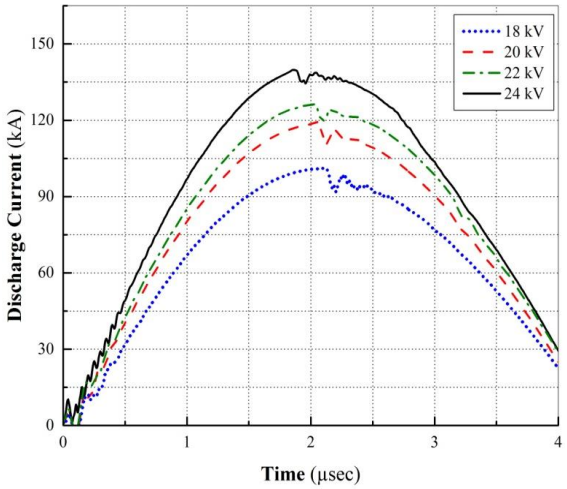

Figure 6. Variation of discharge current with time for argon (All plots are obtained with 0.40 mbar gas pressure).

particles are forced to run away from plasma column. This leads to plasma zone decay. While the plasma column collapses, the accelerated ions move toward the cathode. These ions are collected by FC. In contrast, electrons directed toward anode are decelerated by the effect of the presence of target atoms of anode. These electrons lose their energy in the form of electromagnetic radiations . This phenomena is more responsible for the emission of hard x-rays. In figures 4 and 5, ion flux and hard x-ray intensity of argon gas are shown at four charging voltages in various pressure conditions. According to ion flux graphs, the more charging voltage being applied, the more accelerated ions are collected. The optimum pressure for ion emission in 18, 20, 22 and 24 kV charging voltages was around 0.3, 0.4, 0.5 and 0.6 mbar respectively. The maximum hard x-ray intensity was not simultaneous with ion flux peak. Intense hard x-rays were monitored at pressures around 0.5, 0.6, 0.7 and 0.8 for 18, 20, 22 and 24 kV charging voltages respectively. Similar results had also been reported by Heo et al., [31]. According to the kinetic theory of gases, when gas pressure (or gas temperature) increases, the kinetic energy of gas increases, so it can reach to higher speeds. Therefore, more energetic particles emerge, as a result, more quanta of energy emerges in the form of bremsstrahlung radiations.

3.2. Nitrogen gas

Experiments were repeated for nitrogen gas at the same operating gas pressure and device energy conditions. The discharge current, ion and hard x-ray intensity in different pressure and device energy are depicted in figures 6, 7 and 8, respectively. The discharge current in nitrogen gas was similar to discharge current in–argon gas. But here in nitrogen, the pinch phenomena occur slightly sooner than argon. This observation can be explained by the direct dependence of axial and radial time of the current sheath on the gas density. Optimum pressures with maximum ion beams in ~~the~~ nitrogen were registered around 0.4, 0.5, 0.6 and 0.7 mbar for the studied charging voltages. Hard x-ray intensity in nitrogen also happened later than ion beam signal. The optimal intensity of hard x-ray increased from 0.6 to 0.9 mbar for charging voltage range of 18 to 24 kV. According to the experimental results for both argon and nitrogen gases, the optimum pressure of pinch

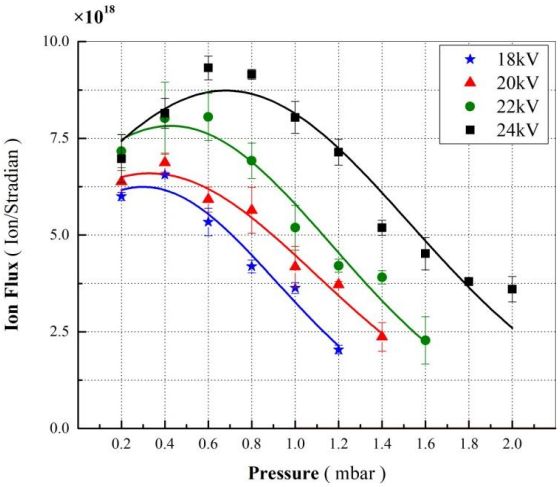

Figure 7. Ion flux variation vs. gas pressure in different charging voltages for nitrogen.

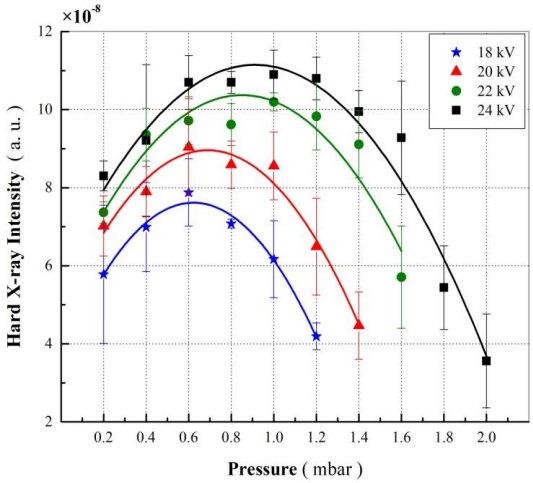

Figure 8. Hard x-ray intensity vs. gas pressure in different charging voltage for nitrogen.

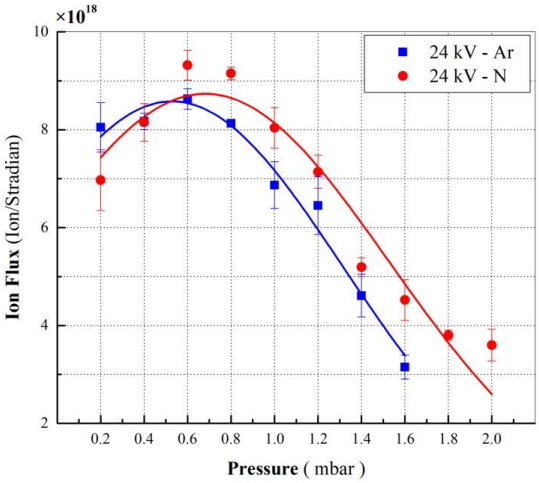

Figure 9. Optimum pressure vs. charging voltage.

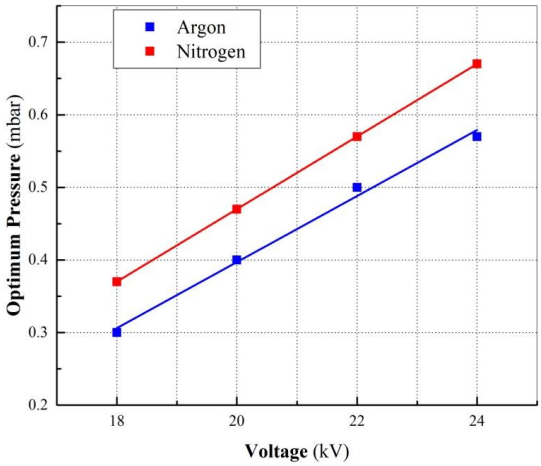

Figure 10. Comparison of ion flux intensity in argon and nitrogen at 24kV charging voltage and 0.40 mbar operating gas pressure.

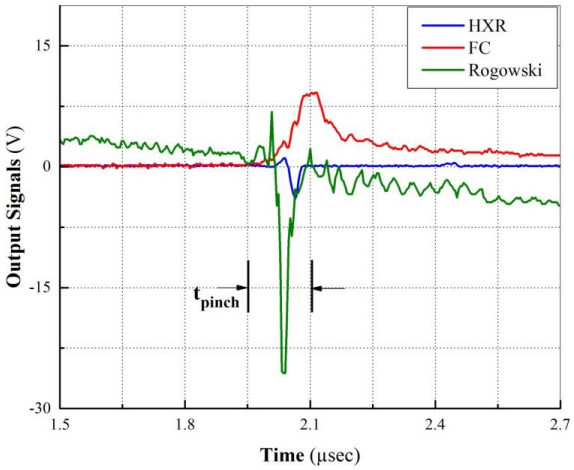

Figure 11. Time characteristics of registered signals by Rogowski coil, Faraday cup and BC-400 scintillation detector.

occurrence, ion flux and hard x-ray emission showed a nearly linear dependence on the charging voltage of the device's capacitor bank. This is depicted in figure 9. Ion flux intensity in nitrogen and argon was compared in figure 10. Before the occurrence of optimum pressure in nitrogen, ion flux in argon was larger than in nitrogen. Because the maximum argon ion flux emission was happening in low pressures. In axial and radial acceleration phases, nitrogen atoms can reach higher speeds than argon ones, so they have more opportunity to reach the Faraday cup. Also, because of lower binding energies of nitrogen electrons than argon electrons, more

nitrogen ions can be created and as a result more charge can be collected by Faraday cup. Time characteristics of the recorded signals from diagnostic tools in nitrogen gas is shown in figure 11 at 22kV charging voltage and 0.40 mbar working gas pressure. A time delay in hard x-ray signal at starting time of the pinch and ion flux signal was monitored. This delay originates from the detector distance from the pinch zone and also it comes from the bremsstrahlung phenomena. According to the plot, ion emission was registered nearly simultaneously with pinch occurrence.

4. Conclusion

In this study the effects of charging voltage of the capacitor bank of PF device (device energy) and the initial pressure of working gas has been investigated on discharge current, ion flux and hard x-ray intensity. This device characteristics were highly affected by the gas's initial pressure as well as device energy. The ion flux for argon and nitrogen gases was in the order of 10^{18} ions per steradian. For a certain charging voltage, ion flux and hard x-ray intensity is increased by increasing ~~in~~ the pressure up to the maximum value at optimum pressure. After this point, the more increase in pressure, the more reduction in experimental amounts. An optimum pressure with maximum ion flux was not the same as the optimum pressure with intense hard x-rays. Hard x-ray intensity reached its peak at higher pressures. Also increasing in device energy enhanced ion flux and hard x-ray intensity. It is concluded that optimum pressure has a nearly linear relationship with charging voltage of the device in both gases. The more voltage was applied to the device's electrodes, the higher current achievements and the sooner pinch happens.

References

1. J W Mather, *Phys. of Fluids* **8** (1965) 366.
2. N V Filippov et al., *Nucl. Fus. Suppl.* **2** (1962) 577.
3. K Takao et al., *Japan. J. Appl. Phys.* **40** (2001) 1013.
4. M J Bernstein, *Phys. Fluids* **13** (1970) 2858.
5. M Mohammadnejad et al., *Rev. Sci. Instrum.* **84** (2013) 073505 .
6. M J Bernstein and G G Comisar, *Phys. Fluids* **15** (1972) 700.
7. T Katsouleas and J M Dawson, *Phys. Rev. Lett.* **51** (1983) 392.
8. M G Heines, *Nucl. Inst. and Methods* **207** (1983) 179.
9. H R Yousefi et al., *Phys. Plasmas* **13** (2006) 114506.
10. S P Gary and F Hohl, *Phys. Fluids* **16** (1973) 997.
11. S P Gray, *Phys. Fluids*, **17** (1974) 2135.
12. Y Mizuguchi et al., *Phys. Plasmas* **14** (2007) 032704.
13. T Haruki et al., *Phys. Plasmas* **13** (2006) 082106.
14. R Deutcch and W Kies, *Plasma Phys. Control. Fusion* **30** (1988) 263.
15. R A Behbahani and F M Aghamir, *Phys. Plasmas* **18** (2011) 103302.
16. R A Behbahani and F M Aghamir, *J. Appl. Phys.***111** (2012) 043304.
17. J N Feugeas et al., *Rad. Eff. Def. Solids* **128** (1994) 267.
18. M Zakaullah et al., *Phys. Plasmas* **6** (1999) 3188.
19. V N Pimenov et al., *Nukleonika* **51**,1 (2006) 71.
20. R S Rawat et al., *Mat. Res. Bull.* **35** (2000) 477.
21. R S Rawat et al., *Surf. Coat. Tech.* **138** (2001) 159 .
22. H Kelly et al., *Plasma Sources Sci. Technol.* **5** (1996) 1.
23. M T Hosseinnejad et al., *J. Fusion Energy* **30** (2011) 516.
24. M Shafiq et al., *Chin. Phys.* B **19**, 1 (2010) 012801.
25. S J Pestehe, et al., *Phys. Plasmas* **21** (2014) 033504.
26. M Hassan et al., *J. Phys.* D*: Appl. Phys*. **40** (2007) 769.
27. H Kelly et al., *IEEE. Trans. Plasma Sci.* **26**, 1 (1998) 113.
28. G R Etaati, et al., *J. Fusion Energy*. **30** (2010) 121.
29. M Bhouyan et al., *Physics of Plasmas,* **18** (2011) 033101.
30. T Yamamoto et al., *Japan. J. Appl. Phys.* **23** (1984) 242.
31. H Heo and D K Park, *Phys. Scr.* **65** (2002) 350.
32. S Lee*, IEEE Trans. on Plasma Sc*. **19** (1991) 912.